Temperature dependence of coercivity of epitaxial magnetic garnet films

M. Pardavi-Horváth
Central Research Institute for Physics, Hungarian Academy of Sciences, H-1525 Budapest 114, P. O. Box 49, Hungary

G. Vértesy
Hungarian Optical Works, H-1525 Budapest, P. O. Box 52, Hungary

(Received 1 February 1985; accepted for publication 15 July 1985)

The temperature dependence of the coercivity H_c, magnetization, anisotropy, and domain wall energy was measured for SmGaYIG, SmCaGeYIG, and SmLuCaGeYIG epitaxial bubble garnet films from 100 K up to the Néel temperature $T_N \gtrsim 400$ K. Data were analyzed together with results published on similar samples on the basis of the theory of domain wall pinning by a random array of uniform defects and a good fit was observed in the form of $H_c^{1/2} = H_0^{1/2} - CT^{2/3}$, where H_0 and C are constants. The maximum average interaction force between defects and walls is 2.9×10^{-7} dyne, corresponding to the minimum interaction range equal to the wall width. The density of defects is in the range between 10^{14} and 10^{16} cm^{-3}. The size and number of defects derived from the temperature dependence of H_c is in agreement with the microstructure of epitaxial garnets revealed by transmission electron microscopy.

I. INTRODUCTION

Epitaxial magnetic garnet films are among the most perfect single crystalline materials, their growth by liquid-phase epitaxy (LPE) technology and control of magnetic properties are well-established processes. Their magnetic domain structure is very simple due to the growth-induced uniaxial anisotropy K_u orienting the magnetization $4\pi M_s$ normal to the surface of the thin garnet film; 180° domain walls are perpendicular to the film surface. Wall separation (1–10 μm) is large compared with the wall width ($\delta \simeq 0.1$ μm), so that interaction between walls is negligible. This domain structure persists up to temperatures near to Néel temperature $T_N \gtrsim 400$ K. Magnetization changes take place via wall motion. These films offer a unique possibility to compare the existing theories with experiment because many of the simplifying assumptions of the theory are valid in this case. The coercivity H_c, i.e., the minimum magnetic field which initiates wall motion, depends on local variations of the wall energy σ due to defects; H_c of epitaxial garnet films varies from ~ 0.1 Oe up to a few oersteds. For bubble-memory device operation a relatively low coercivity is needed: specification requires $H_c < 0.5$ Oe. Over the last few years no small amount of effort has been devoted to revealing the sources of coercivity in garnet films.[1–4] Most of H_c data on bubble garnet films are reported for a limited range around room temperature, where the temperature dependence is linear. A closer look at the published data reporting coercivity values in a wider temperature range[5–13] and our own measurements have shown that garnet film coercivity is a decreasing function of temperature and linearity holds only in a restricted range around room temperature.

Classical theories assume coercivity caused by stress fields, for example, of dislocations.[14] These theories have led to models in which the temperature dependence of H_c is proportional to the wall width. For epitaxial garnets it should give a coercivity increasing with temperature, in disagreement with observation. Träuble[15] derived an expression for H_c taking into account all the possible contributions to H_c from dislocations and inclusions. The temperature dependence of H_c can be approximated by a polynomial $H_c(T) \sim 1/M_s(T) \Sigma_i c_i [K(T)]^{n_i}$, with $-1/4 \leqslant n_i \leqslant 3/2$. Experimental verification and fitting of data to this expression are practically meaningless without exact knowledge of the nature, number, and size of the defects. The assumption that the mechanism of domain-wall pinning, i.e., coercivity, is that walls are bowed between individual pinning sites and break away to the next site when the applied field reaches a critical value was proposed by Kersten in 1956.[16] His calculations give a coercivity proportional to the wall energy, which is a decreasing function of temperature. Previous studies[5,17–19] assumed that domain-wall motion takes place past localized pinning sites, representing energy barriers which can be overcome by the thermal energy, and walls can break away from pinning sites under the simultaneous influence of external field and temperature; however, these models, due to their phenomenological character, cannot give *a priori* values of coercivity.

A microscopic, statistical theory taking into account the properties of the pinning sites was developed by Gaunt.[20] The pinning sites are uniform and are characterized by the maximum restoring force $f = (de/dx)_{\max}$, where e is the interaction energy between a wall and a single pinning site; the pinned area of the wall S depends on the applied field. In zero field $S = S_0 = (4bp)^{-1}$, where $4b$ is the interaction range of the site. Its minimum value is equal to the wall width: $4b_{\min} = \delta$. The critical field required to release the domain walls from the pinning sites of density ρ without thermal activation is $H_0 = f/2M_sS$, the form derived by Kersten.[16] The wall can move across a pinning site by two mechanisms. In the case of "strong" pinning the wall bows out between the pinning sites and at $H = H_0$ it breaks free and moves to the next interacting site. For this case, Eq. 13 of Ref. 20 gives the critical field needed to unpin a wall without thermal activation:

$$H_0 = 0.238 \, (f^2 \rho / M_s \sigma) \, . \tag{1}$$

In the case of "weak" pinning the wall interacts with a ran-

 0021-8979/85/223827-06$02.40

dom array of pinning sites and the statistical fluctuation of the distribution of sites leads to the pinning force and thus to H_c. The maximum value of the critical field for the start of the wall motion is

$$H_0 = 0.258\,(f^2\rho/M_s\sigma)\,. \tag{2}$$

This differs very little from the critical field for strong pinning.

At $T \neq 0$ thermal energy is available to supply the activation energy to break away the wall from its minimum energy position. The required activation energy was calculated in Ref. 20 and the coercivity is given by

$$(H_c/H_0)^{1/2} = 1 - [75kT/(4bf)]^{2/3} \tag{3}$$

for strong pinning. For weak, collective pinning at finite temperatures H_c is equal to

$$H_c/H_0 = 1 - 25kT/(31.0\sigma b^2)\,. \tag{4}$$

In spite of the similarity of the H_0 values for strong and weak pinning, formulas (3) and (4) differ significantly in temperature dependence, thereby enabling comparison with experiments. Among the models this theory of wall pinning can most easily be adapted to the case of epitaxial garnets because all of the parameters of the theory can be derived experimentally. The aim of the present work was to investigate the temperature dependence of coercivity of various bubble garnet films and to get an insight into the properties of the pinning centers: in addition, it may be possible to identify the pinning centers with known defects of epitaxial films.

II. EXPERIMENTS

Measured samples were 2–10-μm-thick garnet films, grown by liquid phase epitaxy on [111]-oriented GGG substrates, with a nominal composition of $(YSm)_3(FeGa)_5O_{12}$, $(YSmCa)_3(FeGe)_5O_{12}$, and $(YSmCaLu)_3(FeGe)_5O_{12}$. The room-temperature coercivity value was usually higher than that for device quality films, so that the relative inaccuracy of the measurements is reduced. Four groups of garnet crystal films were investigated, all based on Sm substituted YIG to ensure the existence of the simple domain geometry. The first group of samples contained Ga for $4\pi M_s$ reduction and had a more pronounced temperature dependence, as the Néel temperature of these films is about 400 K. The second group was substituted with Ca and Ge to raise the Néel temperature above 470 K; these films are known to have higher coercivity (see, e.g., in Ref. 2); the third group of LuSmCaGeYIG films had higher wall energy due to higher anisotropy. Individual films of more exotic compositions were included in the last group if sufficient data were available on the temperature dependence of their properties.

The coercivity was measured using the stripe domain-

TABLE I. Room-temperature magnetization ($4\pi M_s$), anisotropy (K_u), thickness (h), and coercivity (H_c) of epitaxial garnet films. H_0 and C are the parameters of the $T^{2/3}$ fit to Eq. (5).

No	$4\pi M_s$ (G)	K_u (10^3 erg/cm^3)	h (μm)	H_c (Oe)	H_0 (Oe)	C	Ref.
11	204	~10	4.8	0.8	49.2	0.14	
12	205	~10	5.2	0.9	40.7	0.13	
13	229	~10	4.0	1.1	56.8	0.15	
14	170	13	6.7	1.8	23.5	0.08	
15	146	5.8	6.8	0.23	19.5	0.09	13
16	275	16.4	3.9	0.9	19.6	0.08	5
21	143	6.2	5.5	1.4	21.1	0.07	
22	224	7.5	7.6	1.7	204	0.29	
23	200	7.2	5.1	1.8	36.6	0.11	
24	300	5.8	9.2	0.8	5.43	0.036	
25	195	5.7	5.1	2.5	103	0.19	
26	165	4.1	5.8	0.5	16.1	0.07	11
27	98	4.9	6.1	1.1	44.0	0.13	11
31	305	9.04	2.9	1.3	61.8	0.15	
32	168	5.5	6.7	4.8	63.9	0.13	
33	238	14.8	2.85	0.7	15.0	0.065	
34	160	11.0	9.2	0.9	29.1	0.08	
35	350	22.7	2	0.25	8.5	0.05	6
36	490	14.1	1.8	0.33	6.88	0.046	7
37	359	18.0	2.2	0.31	6.39	0.043	7
38	419	32.8	2.5	0.53	7.83	0.046	7
39	234	10.9	5.1	0.13	5.86	0.046	7
40	330	16.4	2.2	0.3	8.8	0.05	8
41	480	13.9	1.8	0.3	6.2	0.05	8
42	237	10.9	~ 5.4	0.12	7.3	0.05	9
43	243	14.1	~ 5.4	0.23	9.1	0.05	9
44	227	12.3	5.1	0.3	6.03	0.04	12
51	352	34.6	13.5	0.5	61.8	0.18	
52	152	6.05	7.4	0.33	33.9	0.12	13
53	144	5.7	6.8	0.2	31.4	0.12	13
54	~700	75	0.94	0.24	3.92	0.03	10

Compositions: Nos. 11–16: SmGaYIG; Nos. 21–27: SmCaGeYIG; Nos. 31–44: LuSmCaGeYIG; No. 51: YbGdBiAlYIG; No. 52: EuGaYIG; No. 53: EuYbGaYIG; No. 54: BiCaSiYIG.

wall oscillation method[21]; that is, the amplitude of an ac field oriented perpendicular to the sample plane was increased linearly from zero, and the field H_c when the domain walls started to move was detected photoelectrically. The saturation magnetization $4\pi M_s$ was calculated using the measured value of the zero field stripe domain period p_0 and the bubble domain collapse field H_{co}[22]; p_0 was measured using the first order diffracted light from the domain pattern[23]; H_{co} was determined using the method described in Ref. 24. The uniaxial anisotropy field H_k was measured magneto-optically.[25] The exchange energy was calculated from the wall energy $\sigma = 4\pi M_s^2 l$ and $\sigma = 4(AK_u)^{1/2}$. The characteristic length l was determined from the value of p_0 and the film thickness h according to Ref. 26. The accuracy of H_c, H_{co}, p_0, and H_k measurements are ± 0.1 Oe, ± 1 Oe, $\pm 0.1\,\mu$m, and ± 10 Oe, respectively.

The temperature of the sample can be varied between 80 and 470 K. The temperature is measured with an accuracy of ± 0.5 K by a thermocouple close to the area of the sample where the optical measurement itself takes place. The sample holder, isolated from its surroundings by a vacuum, can be cooled by a stream of evaporated liquid nitrogen and can be heated by an electric current. Magnetizing coils generating ac and dc fields are built into the sample holder. The beam of the He-Ne laser used for measurements is able to pass through the system.

III. RESULTS

The most important magnetic parameters of the samples from the present work (room temperature values of coercivity H_c, magnetization $4\pi M_s$, uniaxial anisotropy K_u, and films thickness) are summarized in Table I together with data from Refs. 5–13. Data analysis was performed not only on samples measured by us but also on data of similar films taken from the literature.[5–13]

Figures 1–4 illustrate the temperature change of the coercivity and the basic magnetic parameters (magnetization, anisotropy, and wall energy) for typical samples of Table I with room temperature coercivities from 0.5 to 2.5 Oe. Solid curves are drawn through experimental points only to guide the eye. The coercivity of all the measured epitaxial garnets increases with decreasing temperature. Around room temperature the change in H_c is slow and it can be taken as linear, with a temperature coefficient $dH_c/dT \approx -10^{-2}$ Oe/K, as is the practice in bubble material characterization. On decreasing the temperature below about 300 K the coercivity increases monotonically in a nonlinear fashion.

The magnetization, the anisotropy, and the exchange energy have negative temperature coefficients. The bubble-film quality factor $Q = K_u/(2\pi M_s^2)$, which characterizes the stability of the domain structure, also decreases with increasing temperature, but remains higher than unity in the whole temperature range of our investigations. This means that the basic domain structure and the wall-motion magnetization process do not change with temperature. Owing to the higher Néel temperature of CaGe garnets it is expected that the possible effects connected with the lowering of Q are less pronounced in these films around room temperature.

IV. DISCUSSION

For most of the soft magnetic metals and alloys, the coercivity contribution to domain wall motion is scaled with

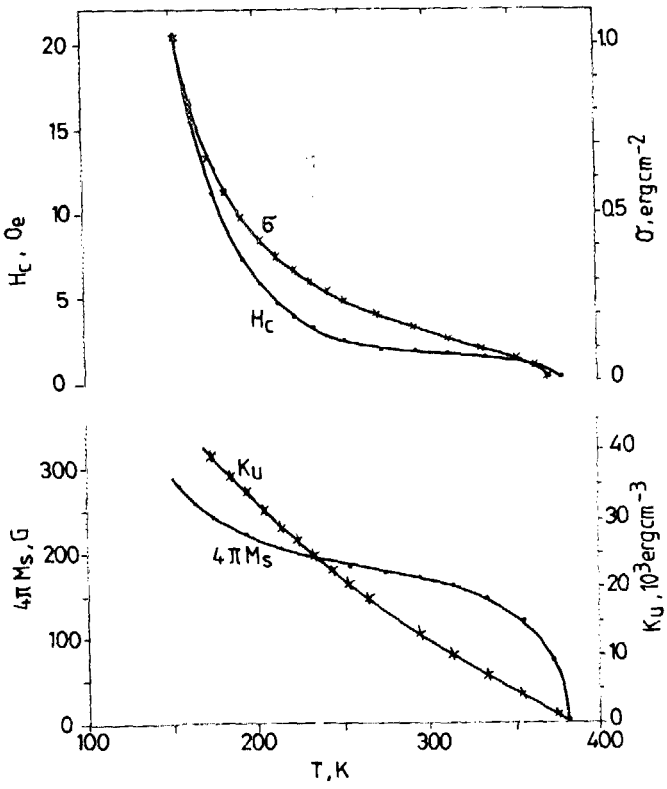

FIG. 1. Temperature dependence of the magnetization $4\pi M_s$, anisotropy K_u, domain-wall energy σ, and coercivity H_c for a SmGaYIG sample (No. 14 of Table I).

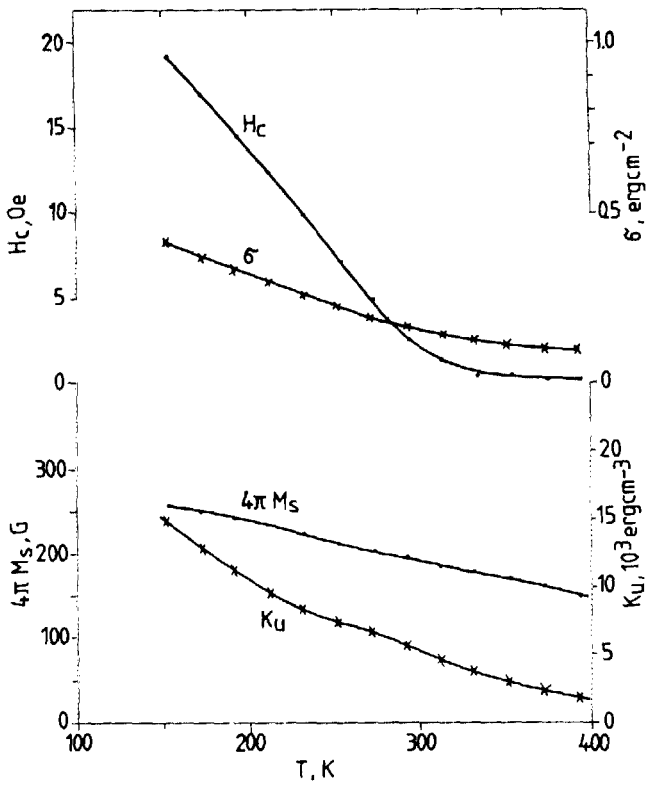

FIG. 2. Same as Fig. 1 except for a SmCaGeYIG sample (No. 25 of Table I).

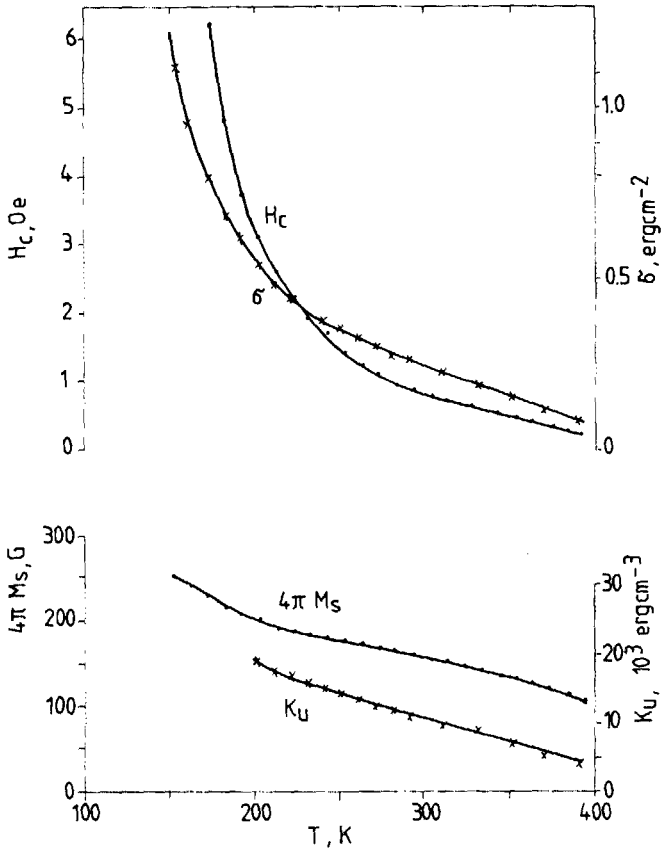

FIG. 3. Same as Fig. 1 except for a SmLuCaGeYIG sample (No. 34 of Table I).

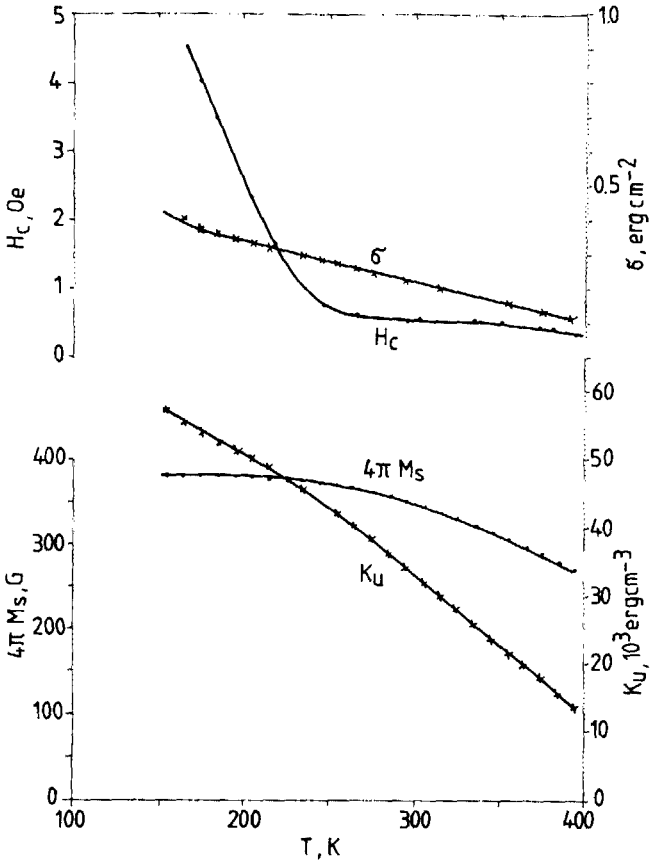

FIG. 4. Same as Fig. 1 except for an YbGdBiAlYIG sample (No. 51 of Table I).

the temperature variation of domain wall width, so H_c increases with temperature. This is definitely not the case with bubble garnets as can be seen in Figs. 1–4. The model of wall bowing of Kersten[16] gives a coercivity proportional to wall energy σ; this seems to be a reasonable result for epitaxial garnets. Figure 1 and 3 indicate that wall energy and coercivity change in a similar manner, although H_c and σ curves are not normalized to each other. On the other hand, the increase of H_c with respect to wall energy is faster for samples of Figs. 2 and 4, so it is unlikely that a simple mechanism of H_c proportional to wall energy would be adequate for the description of the temperature dependence of H_c in epitaxial garnet films. Taking into account the thermal activation model of Ref. 20, a least squares fit to Eq. (3) in the form of

$$H_c^{1/2} = H_0^{1/2} - CT^{2/3}, \tag{5}$$

where

$$C = H_0^{1/2}[75k/(4bf)]^{2/3} \tag{6}$$

gives a good fit from 150 up to 350 K, in some cases even in a wider range of temperatures (for sample No. 32 from 130 up to 430 K). The calculated values of H_0 and C of (6) are given in Table I. Figure 5 gives the $H_c^{1/2}$ vs $T^{2/3}$ curves for the samples of Figs. 2 to 4 and No. 23. Straight lines are the result of the fit to Eq. (5) with H_0 and C given in Table I. Figure 5(a) is a typical curve of a good fit in the 150–350 K range with a correlation $r = 0.99$; this dependence is characteristic of the majority of samples. Figure 5(b) represents de-

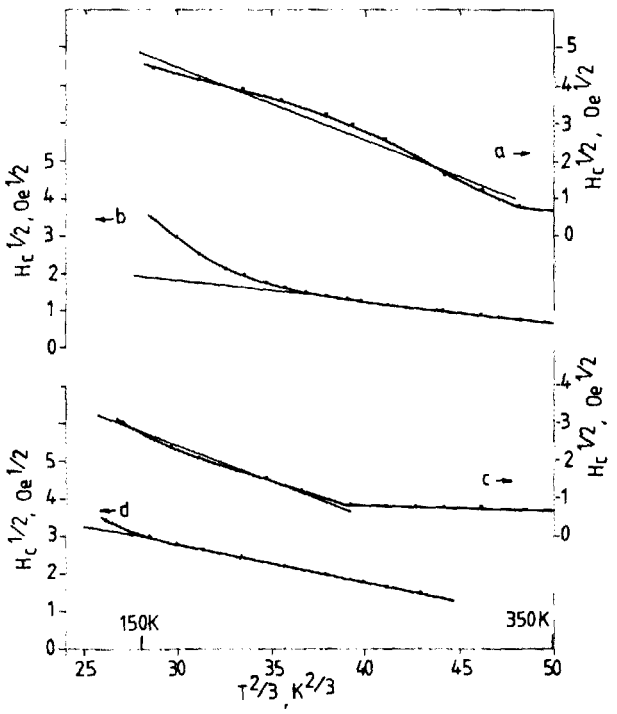

FIG. 5. Temperature dependence of the coercivity in the form $H_c^{1/2}$ vs $T^{2/3}$ (dotted lines); least squares fit to Eq. (5) (solid lines). Curves: (a) sample No. 25; (b) No. 34; (c) No. 51; and (d) No. 23.

viation from the $T^{2/3}$ fit at decreasing temperatures; Fig. 5(c) corresponds to the situation where the decrease of H_c is very slow for $T^{2/3}$ at $T > 300$ K.

For all $H_c(T)$ dependencies measured by us and published in Refs.[5–13], the $T^{2/3}$ law seems to be valid at least between 150 and 350 K with a correlation factor of the least squares fit better than 0.97. At the low-temperature limit the increase of the coercivity is stronger than the predicted $T^{2/3}$; at the high-temperature limit H_c decreases with T practically linearly, a feature that may be connected with the temperature variation of the interaction energy between defects and domain walls.

Whereas the room temperature values of H_c vary an order of magnitude, the H_0 values span two orders of magnitude (from 4 to 200 Oe). The scatter of coefficients C is small again, especially when one looks at $C' = C H_0^{-1/2} = [75k/(4bf)]^{2/3}$ values which range from 0.015 to 0.023 with a mean value of 0.018 ± 0.002 giving $4bf = 4.3 \times 10^{-12}$ erg. This means that either the interaction force between defects and the interaction range remains nearly constant for all epitaxial garnets or $4bf$ is a constant; however, Gaunt's theory[20] assumes that b and f are independent variables. The minimum interaction range for the model $4b_{\min}$ is equal to the wall width. For a typical case where $\delta = 0.15\,\mu$m, this leads to the maximum interaction force of $f_{\max} = 2.9 \times 10^{-7}$ dyne. Assuming $4b = \delta$, the interaction forces for all but two samples of Table I were computed leading to f in the range from 2×10^{-7} dyne up to 4×10^{-7} dyne. Sample Nos. 38 and 54 have the exceptionally high f values of 6.4×10^{-7} and 9.7×10^{-7} dyne, respectively.

The constancy of $4bf$ indicates that the character and type of the pinning centers is the same for all garnet films of the present work. As the technique of LPE growth is a well-established process and practically the same in every laboratory and since the films of Table I represent standard bubble materials, it is reasonable to assume the same type of defects exist in most bubble films.

From Eqs. (1) and (2), $f^2\rho$ can be computed:

$$f^2\rho \simeq M_s \sigma H_0 / 0.25 . \tag{7}$$

The scatter in corresponding $f^2\rho$ values is much greater than in bf values. $f^2\rho$ is in the 10^2–10^3 dyne^2/cm^3 range, with maximum $f^2\rho$ of 2620 and minimum of 70 dyne^2/cm^3 for samples No. 22 and No. 24, respectively. From the known f values the defect densities can be determined. The order of magnitude of ρ varies from 10^{14} cm^{-3} to 10^{16} cm^{-3}, according to the variation of $f^2\rho$ mainly caused by H_0 changes. Such densities may have defects which have a maximum size of 10^{-5} cm.

Usual optical and SEM investigations do not show any sign of such a high-defect density. In spite of the relatively high H_c, the samples have a very small number of dislocations and surface irregularities. These defects could result in localized pinning of some walls that does not affect the average H_c measured photoelectrically on a large number of walls. The high density of defects derived from the temperature dependence of coercivity can only have its origin in the microstructure of LPE garnets inaccessible to usual characterization methods. Transmission electron microscopy (TEM) is capable of revealing these defects whose existence was already supposed.[18]

Judging from our TEM data on epitaxial garnets, partly published in Refs. 3 and 4, the microstructure of LPE garnet films of the same composition type is remarkably similar. Two basic types of microstructure can be distinguished. The first is a periodic composition modulation which creates a periodic stress field due to the corresponding lattice parameter variations.[3] The period of the three-dimensional pattern is $\Lambda = 5 \times 10^{-6}$ cm for a bubble film from the same growth series as No. 23. The defect density $\rho = \Lambda^{-3} = 8 \times 10^{15}$ cm^{-3} is in agreement with $\rho = 6.4 \times 10^{15}$ cm^{-3} for sample No. 23. For this sample a very good fit with $r = 1.00$ to the $T^{2/3}$ function was obtained and given in Fig. 5(d). The calculated values of the parameters of the model are $f^2\rho = 356$ dyne^2/cm^3 and $bf = 10.6 \times 10^{-13}$ erg leading to $f = 2.4 \times 10^{-7}$ dyne for $b_{\min} = 4.5 \times 10^{-6}$ cm. It can be concluded that one of the causes of wall pinning in dislocation-free LPE garnets is connected with this type of microstructural defect.

Another type of microstructure in the form of small precipitates was observed in garnet films with a tendency towards higher coercivity: in some samples small spherical precipitates are present with a typical size of less than 10^{-5} cm and a density of the order of 10^{17} cm^{-3}. According to STEM-EDX data their composition differs from the matrix in Y/Ca ratio.[4] The exact nature of these crystalline defects is under investigation. However, the defect densities observed in TEM are in accordance with the computed values from the temperature dependence of coercivity assuming a thermal activation mechanism and strong pinning.

The consistency of the experimental data with Gaunt's model is intriguing because the model does not take into account the temperature dependence of the magnetization, wall width, wall energy, and interaction energy. These quantities change substantially in the temperature range of our investigations. From 200 to 300 K, M_s decreases nearly 4 times (see, e.g., No. 34 in Fig. 3). If $f^2\rho$ were independent of T then we could observe an increase of the (extrapolated to 0 K) H_0 value by a factor of two [for sample No. 34 in Fig. 5(b)]. For this temperature range experimental data follow the $T^{2/3}$ law well; towards lower temperatures, deviation from linearity is pronounced which can be taken as an increase of H_0 with decreasing temperature. On the other hand, this may be a sign of the slowing down of the change of f caused by the increased stiffness of the walls connected with the rapidly increasing anisotropy energy. A constant H_0 in a wide temperature range may be observed if the temperature variation of M_s is compensated by that of $f^2\rho$. It is not likely that ρ changes; therefore f^2 has to be decreased by the same amount as σM_s on increasing the temperature. For the above example f has to decrease by twice its original value from 200 to 300 K, that is, by 0.5 % K^{-1}. One can speculate that on increasing the temperature the interaction energy is decreased until it falls into the "weak" pinning mode about room temperature and gives rise to the linear temperature dependence of H_c. This very simplified argument does not take into account the decrease of Q in establishing the observed behavior of H_c.

V. CONCLUSIONS

The coercivity of epitaxial garnet films increases very rapidly below room temperature. Linearity of H_c vs T curves could be observed in a limited temperature range above 350 K. The form of temperature dependence corresponds to the statistical theory of the domain wall pinning aided by thermal activation.[20] The basic parameters of the theory were evaluated from the experimental data. The critical field (H_0) for wall motion in the absence of thermal activation varies between 4 and 200 Oe for the room temperature values of H_c between 0.2 and 4.8 Oe. The mean interaction force between the defects and walls is $\bar{f}_{max} = 2.9 \times 10^{-7}$ dyne if the range of interaction $4b_{min}$ is taken to be equal to the domain wall width. Corresponding defect densities are between 10^{14} and 10^{16} cm^{-3}. The practically constant value of $4bf = 4.3 \times 10^{-12}$ demonstrates that in spite of the different origins of the samples in Table I the identity of the growth kinetics of LPE garnet films determines the type of microstructural defects whose number may differ between samples due to the fluctuations in the growth process. Our TEM investigations[3,4] have revealed the existence of various types of microstructure in LPE garnet films. The size and density of the observed precipitates and a periodic composition modulation are in agreement with the above data derived from the temperature dependence of the coercivity with the help of the strong pinning model of the thermally activated, bowed domain walls.

ACKNOWLEDGMENTS

The authors are indebted to Dr. B. Keszei and Dr. J. Vandlik for growing the samples.

[1] M. Pardavi-Horváth, Prog. Cryst. Growth Charact. **5**, 175 (1982).
[2] M. Pardavi-Horváth, M. Balaskó, and G. Vértesy, J. Magn. Magn. Mater. **41**, 315 (1984).
[3] M. Pardavi-Horváth, Á. Cziráki, I. Fellegvári, G. Vértesy, J. Vandlik, and B. Keszei, IEEE Trans. Magn. **MAG-20**, 1123 (1984).
[4] Á. Cziráki, M. Pardavi-Horváth, I. Fellegvári, K. Wetzig, and G. Zies, in *Proc. 8th European Congress on Electron Microscopy*, edited by Á. Csanády, P. Röhlich, and D. Szabó (Progr. Committee, Budapest, Hungary, 1984), Vol. II, p. 965.
[5] P. Pougnet, H. Jouve, and B. Barbara, J. Magn. Magn. Mater. **27**, 109 (1982).
[6] B. Ferrand, H. Moriceu, D. Challeton, and J. Daval, IEEE Trans. Magn. **MAG-14**, 415 (1978).
[7] W. R. Cox and S. G. Parker, Mater. Res. Bull. **13**, 501 (1978).
[8] S. G. Parker and W. R. Cox, J. Crystal Growth **42**, 334 (1977).
[9] G. G. Summer and W. R. Cox, AIP Conf. Proc. **34**, 157 (1976).
[10] S. E. G. Slusky, J. E. Ballintine, R. A. Lieberman, L. C. Luther, and T. J. Nelson, IEEE Trans. Magn. **MAG-18**, 1286 (1982).
[11] S. Bornmann, P. Görnert, V. A. Bokov, M. V. Bistrov, and V. A. Yatsenko, Solid State Phys. (USSR) **21**, 3687 (1979).
[12] R. E. Fontana, Jr. and D. C. Bullock, AIP Conf. Proc. **34**, 170 (1976).
[13] R. M. Sandfort, R. W. Shaw, and J. W. Moody, AIP Conf. Proc. **18**, 237 (1973).
[14] J. Vicena, Czech. J. Phys. **5**, 480 (1955).
[15] H. Träuble, in *Moderne Probleme der Metallphysik*, edited by A. Seeger (Springer, Berlin, 1966), p. 376.
[16] M. Kersten, Z. Angew. Phys. **8**, 496 (1956).
[17] J. A. Baldwin, Jr., F. Milstein, R. C. Wong, and J. L. West, J. Appl. Phys. **48**, 2612 (1977).
[18] J. Magnin, H. Jouve, and B. Barbara, J. Appl. Phys. **50**, 1538 (1979).
[19] S. Shiomi, S. Iwata, S. Uchiyama, and T. Fujii, IEEE Trans. Magn. **MAG-15**, 930 (1979).
[20] P. Gaunt, Philos. Mag. B **48**, 261 (1983).
[21] J. A. Seitchik, W. D. Doyle, and G. K. Goldberg, J. Appl. Phys. **42**, 1272 (1971).
[22] D. C. Fowlis and J. A. Copeland, AIP Conf. Proc. **5**, 240 (1972).
[23] R. D. Henry, IEEE Trans. Magn. **MAG-13**, 1527 (1977).
[24] M. Balaskó and M. Pardavi-Horváth, Appl. Phys. **16**, 75 (1978).
[25] R. M. Josephs, AIP Conf. Proc. **10**, 286 (1972).
[26] C. Kooy and U. Enz, Philips Res. Rep. **15**, 7 (1960).